



European Commission  
Research Programme of the Research Fund for Coal and Steel

Technical Group: TGA2

Grant Agreement 101033991



**Holistic Assistance for Cross-Process Analysis and Prediction of  
Strip and Plate Flatness**

Deliverable: D2.2

Title: Description of the used first principal models

Lead beneficiary: VDEh-Betriebsforschungsinstitut (BFI)

Authors: Alex Dunayvitser, Nils Hallmanns, Roger Lathe,  
Hagen Krambeer, Andreas Wolff, Fillippo Avellino,  
Unai Argarate

Type: Report

Dissemination level: Confidential

Date of delivery: 30.11.2022

# 1 Index

- 1 Index ..... 2
- 2 Roll gap four/two high mills ..... 4
  - 2.1 General description of the model ..... 4
  - 2.2 References/source of the model..... 5
  - 2.3 Quality of calculations ..... 5
  - 2.4 Influence on Flatness..... 5
  - 2.5 Table of input and output data ..... 6
- 3 Thermal crown of the rolls ..... 8
  - 3.1 General description of the model ..... 8
  - 3.2 References/source of the model..... 10
  - 3.3 Quality of calculation..... 11
  - 3.4 Influence on flatness ..... 12
  - 3.5 Table of input and output data ..... 12
- 4 Coiling and de-coiling model ..... 14
  - 4.1 General description of the model ..... 14
  - 4.2 References/source of the model..... 19
  - 4.3 Quality of calculation..... 19
  - 4.4 Influence on flatness ..... 20
  - 4.5 Table of input and output data ..... 20
- 5 Rheological model ..... 21
  - 5.1 General description of the model ..... 22
  - 5.2 References/source of the model..... 23
  - 5.3 Quality of calculations ..... 24
  - 5.4 Influence on flatness ..... 24
  - 5.5 Table of input and output data ..... 24
- 6 Plate temperature evolution model..... 26
  - 6.1 General description of the model ..... 26
  - 6.2 References/source of the model..... 30
  - 6.3 Quality of calculations ..... 30
  - 6.4 Influence on Flatness..... 30
  - 6.5 Table of input and output data ..... 30
- 7 Roll wear model..... 37



- 7.1 General description of the model ..... 37
- 7.2 References/source of the model..... 38
- 7.3 Quality of calculations ..... 38
- 7.4 Influence on Flatness..... 39
- 7.5 Table of input and output data ..... 39
- 8 Analytic forming model of levelling process ..... 41
  - 8.1 General description of the model ..... 41
  - 8.2 References/source of the model..... 45
  - 8.3 Quality of calculation results ..... 45
  - 8.4 Influence on flatness ..... 45
  - 8.5 Table of input and output data ..... 45

## 2 Roll gap four/two high mills

The following abstract describes the first principal model for the calculation of the roll gap for a four-high stand system. All the equations derived for the system can be used analogously to a lesser extent to describe the two-high stand system. The four-high stand system is more complex and will be explained in detail, but for the two-high mills system it is ultimately the same, and hence only explicit differences of the model will be highlighted.

### 2.1 General description of the model

The model is used to simulate the influence of the bending of the work roll on the shape of the roll gap in a four-high stand system, that can be seen in Figure 1. The shape of the roll gap has a direct impact on the thickness profile of the produced steel plate, e.g., the forming of the crown thickness profile (Figure 2).

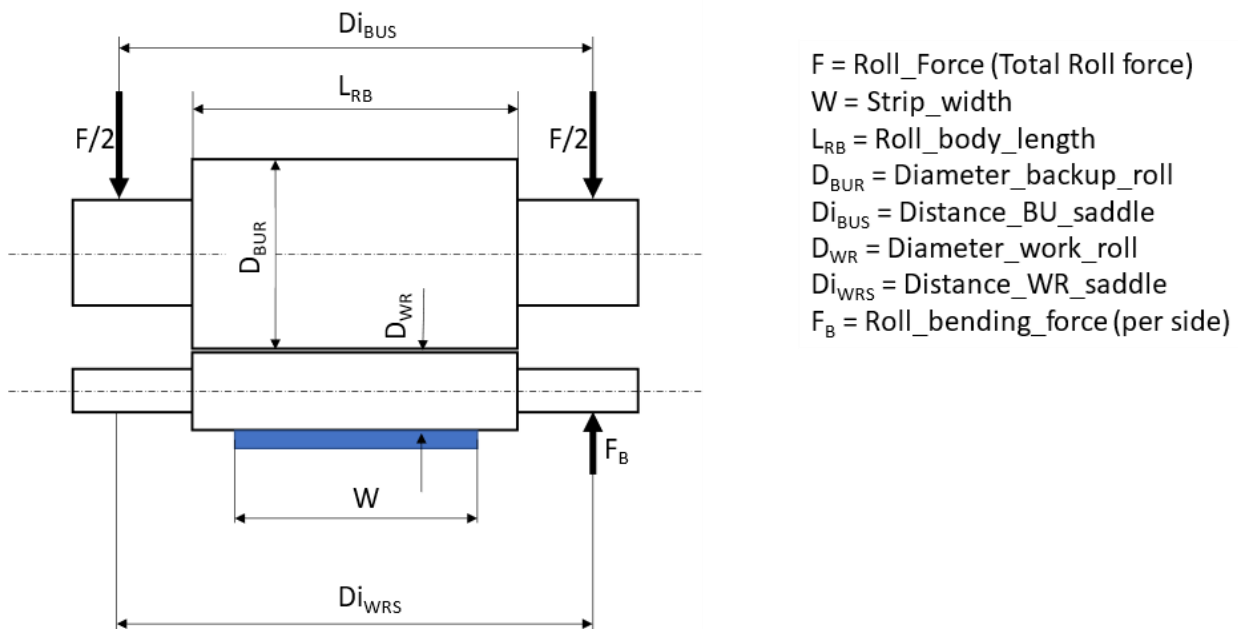
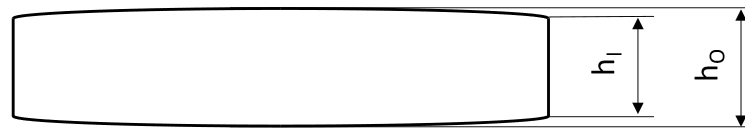


*Figure 1 - Scheme of one half of the four-high mills system, which is used in the model.*

The elasticity theoretical analysis shows that in addition to the known deformations of basic bending theory, further deformation origins must be considered for a sufficient prediction of the roll gap. The major contributions are generated from the bending moment, shear distortion and the roll compression. Considering all these factors calculations are derived which yield the bending of the rolls for a pressure that is distributed arbitrarily on the roll body. These equations are then used to obtain the pressure between work and back up roll and subsequent also the roll gap with corresponding coefficients. If the system of interest is a two-high mill, then there is no backup roll and the work roll has a larger diameter. Hence all the parameters which are used to describe the backup roll or the interaction between work and backup roll become no longer necessary for the calculation of the roll gap.



Thickness profile crown

*Figure 2 - Typical forming of the thickness profile during the rolling process due to roll gap deformation.*

Since some of the systems of equations cannot be solved directly, some approximations have been used which makes it possible to receive the pressure distribution between work and backup roll, the deformation of the roll gap and the crown thickness profile with explicit equations. E.g., for this approximation was assumed, that the pressure in the roll gap is constant and the pressure between the work and back up roll is parabolic.

In case CVC rolls are used the roll crown must be set to zero for work roll and backup roll. After that the change in the roll gap due to the horizontal displacement of the CVC must be calculated and the result must be added to the calculated roll gap. The frequently given CVC “equivalent of roll crown” should not be used as roll crown input for the work and backup roll.

## 2.2 References/source of the model

The theory of the model is extracted from the PHD-thesis [1] about the elastic deformation of four high mills and its influence on the shape of the roll gap. The approximation which is used for the model is also derived in this thesis. The remaining steps for creating the first principal model were made internally at BFI.

[1] Berger B. (1975) Die elastische Verformung der Walzen von Quarto-Walzgerüsten und die Beeinflussung der Walzspaltform durch Walzenbiegeeinrichtungen (The elastic deformation of the rolls of the rolls from the four-high stand system and the influence of roll bending devices on the roll gap shape)

[2] ] European Commission EUR 15517 Neuschütz E., Lathe R., Thies H. (1990) Beeinflussung des Dickenprofils beim Warmbandwalzen (Influencing the thickness profile during hot strip rolling).

## 2.3 Quality of calculations

Since the origin of the model is the PHD-thesis and in there the resulting values match the measurements, the foundation of the model has been tested sufficiently. Because of these past experiences and the relatively small, expected uncertainties on the input variables, the quality of the predicted roll gap is secured.

## 2.4 Influence on Flatness

The roll gap shape directly determines the shape of the thickness profile of the rolled strip for larger strip thicknesses. Investigations [2] have shown that the limit until which the thickness profile is influenced is approx. 10 mm strip thickness. Until this strip thickness there is at the same time no influence on the strip flatness. However, this is not to be seen as a hard limit. However, the test results have shown that below this strip thickness the thickness profile (except for the area near the strip edge) remains almost unchanged. Below this strip thickness, however, a change in the roll gap shape then has the effect of influencing the resulting strip flatness.

In the roughing mill and the first stands of the finishing line of a hot strip mill, a certain thickness profile is produced due to the roll gap shape of the respective stands. Typically, the limit of 10 mm is reached after stand 2 or 3 of the finishing line.

The generated thickness profile remains constant from the 2nd or 3rd stand onwards. Specifically: The relative thickness profile. If, for example, the strip is 1% thicker in the centre than at the edge, then this ratio of 1% centre to edge is maintained in the subsequent passes.

Below the strip thickness of approx. 10 mm, a deviation between the roll gap shape and the relative thickness profile causes a change in the strip flatness. The effect on the strip flatness becomes greater the thinner the strip. It is therefore necessary from this strip thickness downwards to adjust the roll gap in such a way that the roll gap shape and thickness profile match as closely as possible. This is achieved, for example, by adjusting the roll bending and adjusting the CVC rolls. This also applies in particular to the subsequent process step cold rolling. However, if the thickness profile deviation is very large, these adjustment options may be not large enough and the thickness profile deviation results in an unflat strip.

Another aspect is the influence of the thickness profile on the flatness influence during coiling. Here it can generally be said that the larger the thickness profile deviation, the larger the change in strip flatness generated during coiling.

## 2.5 Table of input and output data

All the variables used as an input for the calculation of the roll gap are listed in the table below. The table contains information about the data type, an example input that can be used to run the model and the corresponding unit. As an output the roll gap is calculated with respective coefficients. For the two-high mill all the inputs used to describe the backup roll or the interaction between work and backup roll become no longer necessary.

*Table 1 - Input data for the roll gap model*

Input data	Format / Info	Example input	Unit
Roll_Force $F$	double	5000	kN
Strip_width $W$	double	1400	mm
Entry_thickness	double	5	mm
Exit_thickness	double	4	mm
Roll_body_length $L_{RB}$	double	1800	mm
Diameter_backup_roll $D_{BUR}$	double	1150	mm
Crown_backup_roll	double / NOTE: Please consider remark at bottom.	0	$\mu\text{m}$
Distance_BU_saddle $Di_{BUS}$	double	2200	mm

<b>Diameter_work_roll <math>D_{WR}</math></b>	double	450	mm
<b>Crown_work_roll</b>	double / NOTE: Please consider remark at bottom.	0	$\mu\text{m}$
<b>Distance_WR_saddle <math>Di_{WRS}</math></b>	double	2200	mm
<b>Roll_bending_force <math>F_B</math></b>	double	0	kN
<b>Pointer for Error_code</b>	Adress to pre-allocated INT 32 value		
<b>Pointer for roll_gap</b>	Adress to pre-allocated array of 50 double values		
<b>Vector_length_rollgap</b>	INT 32 (Value = Always 50)	50	
<b>Pointer for relevant_coefficients</b>	Adress to pre-allocated array of 5 double values		
<b>Vector_length_coeff</b>	INT 32 (Value = Always 5)	5	

Table 2 - Output data for the roll gap model

Ouput data	Format/Info	Example output
<b>roll gap</b>	array of length 50 containing doubles	[-0.006,...,-164.087]
<b>relevant_coefficients</b>	Double / Tschebyschew polynom coefficient order = 2	-76.9741
	Double / Tschebyschew polynom coefficient order = 4	-4.56661
	Double / Tschebyschew polynom coefficient order = 6	-2.99692
	Double / Tschebyschew polynom coefficient order = 8	-1.74939
	Double / Tschebyschew polynom coefficient order = 10	-0.868383

### 3 Thermal crown of the rolls

The thermal crown model available at BFI was implemented for the first time as part of the German NRW project blade strip [1]. For the thin strip casting process to be modelled there, the model, described in [2,3] was extended from 2D to 3D. The implementation was done in Matlab and served as a sub-model for the offline simulation of the thin strip casting process for the development of a control strategy for thickness profile and flatness of the strip.

In the HatFlat project, the core of this model was further used. The necessary adjustments essentially consider the CVC displacement of the work rolls and the temperature influence of the back-up rolls. The third dimension, which considers the temperature distribution in the direction of roll rotation, could be omitted and some optimisations were made to the data processing within the model.

#### 3.1 General description of the model

The model was implemented in the programming language c and compiled into a dynamic link library (dll) that can be called with the corresponding interface of Python or LabVIEW.

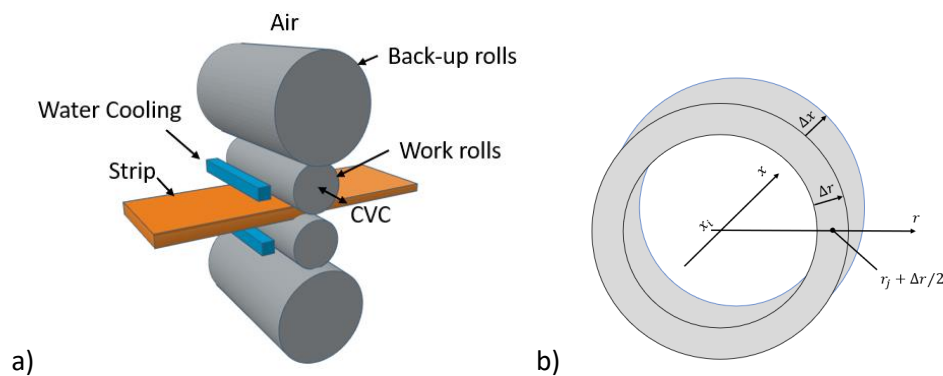


*Figure 3. a) Rolling mill components to be considered in the thermal crown model, b) Circular ring of roll*

Figure 3a shows a rough layout of a quarto mill stand with its work and back-up rolls, as well as a schematically indicated work roll cooling system. The contact between the warm strip and the cooler work roll causes a heat transfer into the work roll. Within the work roll, the increased shell temperature leads accordingly to a heat flow in the direction of the roll core. The heating is counteracted by heat dissipation to the back-up rolls, to the water-cooling systems and to the environment. The temperature distribution within the roll in axial and radial direction leads to a thermal expansion of the roll body. The resulting crown of the rolls has a direct influence on the roll gap and thus on the thickness profile and flatness of the rolled strip. On the other hand, the roll gap geometry is actively influenced by the axial displacement of the work rolls provided with a special crown. This changes the contact zones between the working roll and the strip, as well as the cooling and the back-up roll, which is also considered in the thermal crown model.

For the modelling of the thermal crown model, basically [2] is followed, except for specific adaptations in this project. According to [4,5], the differential equation of the temperature field in the cylindrical coordinate system expanded by the  $z$ -coordinate is as follows:

$$\frac{\partial T}{\partial t} = \alpha \left( \frac{\partial^2 T}{\partial r^2} + \frac{1}{r} \frac{\partial T}{\partial r} + \frac{\partial^2 T}{\partial z^2} \right)$$

*Eq. 3-1*

First, a cylindrical roll is divided in axial direction into slices with thickness  $\Delta x$  and in radial direction into concentric rings with thickness  $\Delta r$ . In rolling processes, the x-coordinate is always reserved for the width direction, which corresponds to the z-coordinate in cylindrical coordinates. Figure 3a shows a circular ring with the corresponding coordinates. For the calculation of the heat balance, the areas between the elements must be considered. The area of the outer surface of a circular ring is:

$$S_j = 2\pi \left( r_j + \frac{\Delta r}{2} \right) \Delta x$$

*Eq. 3-2*

The area of the face of a circular ring is:

$$A_j = \pi \left( r_j + \frac{\Delta r}{2} \right)^2 - \pi \left( r_j - \frac{\Delta r}{2} \right)^2 = 2\pi r_j \Delta r$$

*Eq. 3-3*

With the volumes of the circular rings:

$$V_j = A_j \Delta x$$

*Eq. 3-4*

the masses give in to them:

$$m_j = V_j \rho$$

*Eq. 3-5*

The temperature change for the circular rings results from its heat capacity and the heat flow admitted or dissipated:

$$\dot{T}_{i,j} = \frac{1}{m_j c} \dot{q}_{i,j}$$

*Eq. 3-6*

The heat flows  $\dot{q}_{i,j}$  pass between the individual elements through their common surfaces. The temperature difference between two neighboring elements drives the heat flow through their common surface along the element length with the thermal conductivity of the material. In the width direction x, the heat flows result in:

$$\dot{q}_{i \rightarrow i+1, j} = -k \frac{A_j}{(x_{i+1} - x_i)} (T_{i+1, j} - T_{i, j})$$

*Eq. 3-7*

and in a radial direction:

$$\dot{q}_{i, j \rightarrow j+1} = -k \frac{2\pi \Delta x}{\ln \left( \frac{r_{j+1}}{r_j} \right)} (T_{i, j+1} - T_{i, j})$$

*Eq. 3-8*

The total balance of heat flows for a circular ring inside the cylinder is given by:

$$\dot{q}_{i,j} = \dot{q}_{i-1 \rightarrow i,j} - \dot{q}_{i \rightarrow i+1,j} + \dot{q}_{i,j-1 \rightarrow j} - \dot{q}_{i,j \rightarrow j+1}$$

*Eq. 3-9*

Heat exchange with the environment takes place on the outer rings of the cylinder with the index  $je$ :

$$\dot{q}_{i,je \rightarrow 0} = -h_0 S_{i,je} T_0 - T_{i,je}$$

*Eq. 3-10*

Coefficient  $h_0$  and temperature  $T_0$  stand for the heat transfers between strip, water, and air with the rolls ( $h_s, h_w, h_a, T_s, T_w, T_a$ ).

In contrast to the literature [1,2], several simplifications have been made here regarding different material properties. In contrast, a significantly larger number of elements is used, especially in the width direction, to better represent the CVC shifting of the work rolls and the swarming of the strip in the width direction. The grid width  $\Delta x$  is valid for the work rolls, the back-up rolls, the strip, and the water-cooling systems. Due to the finer grid, a consideration of full elements is sufficient. After the calculation of the heat exchange, the temperature field in the roll can be recalculated with the time step  $\Delta t$ :

$$T_{i,j}(t) = T_{i,j}(t - \Delta t) + \frac{1}{m_{i,j} c_{i,j}} \dot{q}_{i,j} \Delta t$$

*Eq. 3-11*

According to [2], the thermal crown is calculated from the temperature field using thermal expansion coefficient:

$$u_i = \frac{2}{r_{je}} \beta \sum_{j=1}^{je-1} (T_{i,j} - T_e) \left( r_j + \frac{\Delta r}{2} \right) \Delta r$$

*Eq. 3-12*

In the total crown model, the calculation is basically carried out for work rolls and back-up rolls. The specific roll parameters and the different contact conditions are passed to the sub-model.

## 3.2 References/source of the model

- [1] Land NRW Projekt; Innovative Werkstoffgeneration für Schneidwaren durch die zukunftsweisende Fertigungstechnologie Bandgießen (BladeStrip); Förderkennzeichen 005-1009-0056; ThyssenKrupp Nirosta GmbH (TKN), Ernst Krebs KG (Krebs), VDEh- Betriebsforschungsinstitut GmbH (BFI), Max-Planck-Institut für Eisenforschung GmbH (MPIE), 01.05.2011 – 30.04.2014
- [2] A. M. Campos, D. F. García, R. Usamentiaga N. de Abajo, J. A. González; A Real-time Thermal Model for the Intelligent Control of Cooling Systems for Hot Strip Mill Work Rolls; University of Oviedo Campus de Viesques; Aceralia Steel Corporation Centro de Desarrollo Tecnológico; Asturias, 2000

- [3] A. M. Campos, D. F. García, Member, IEEE, N. De Abajo, and J. A. González; Real-Time Rule-Based Control of the Thermal Crown of Work Rolls Installed in Hot Strip Mills (IEEE TRANSACTIONS ON INDUSTRY APPLICATIONS, VOL. 40, NO. 2, MARCH/APRIL 2004)
- [4] E. Schmidt, Einführung in die Thermodynamik, Springer-Verlag, Berlin / Göttingen / Heidelberg 1958
- [5] A. Bejan, A.D. Kraus, Heat Transfer Handbook, Duke University Durham, North Carolina, University of Akron, Ohio, John Wiley & Sons, Hoboken, New Jersey 2003

### 3.3 Quality of calculation

The signal flow diagram in Figure 4 shows the sequence of calculations from the temperature distribution in a work roll body. The temperature field is used in the calculation of the heat flows within the body and with peripheral components for the resulting temperature field change. After integration, the thermal crown is calculated with the new temperature field. In principle, this sequence applies equally to a back-up roll, with the special feature that there is no contact with the strip. The entire process is calculated cyclically, for example every one second.

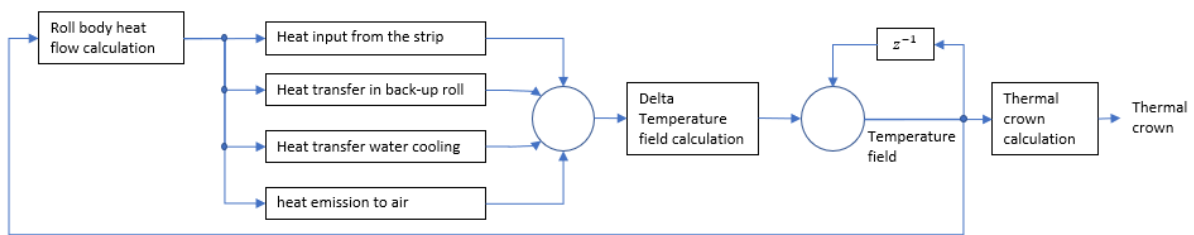
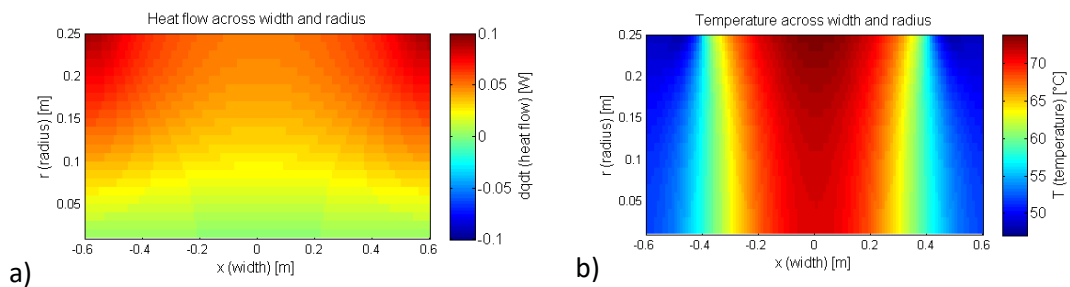
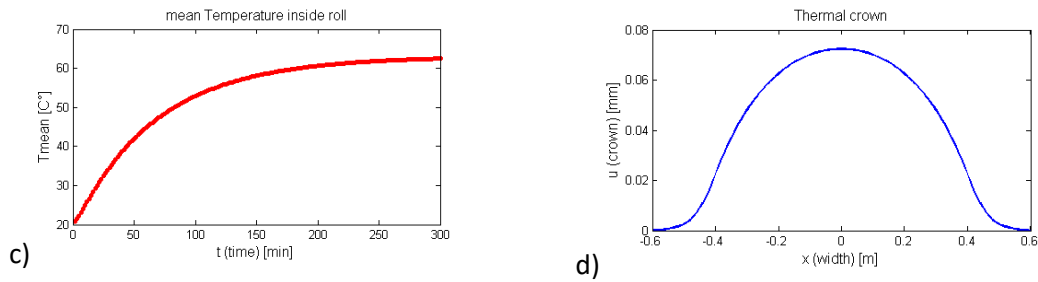


Figure 4. flow chart of thermal crown calculation for one work roll

Figure 5 shows outputs of the model after an example simulation. It has been started with a homogeneous temperature distribution 20°C in the roll and a strip with a constant temperature of 800°C. In a) the heat flows, in b) the temperature distribution, in c) the time course of the mean temperature and in d) the resulting thermal crown of the work roll are shown.





**Figure 5.** Simulation example: work roll heating after one hour started at 20°C and strip temperature at 800°C: a) Heat flow, b) Temperature, c) Evolution of the mean temperature inside roll body, d) thermal crown

To adapt the model to the rolling stands to be simulated in this project, calibration procedures are carried out, especially regarding the determination of the heat transfer coefficients to the peripheral plant parts. First, existing plant parameters are adopted, then the parameters are optimized step by step by means of process identification. Other parameters, such as all geometric dimensions, but also the specific density, heat capacity and thermal conductivity of the roll materials can be specified very precisely in advance. Important reference variables for the first model test are the directly manually measured surface temperature profile and thermal crown of the rolls, before and after removal.

### 3.4 Influence on flatness

The thermal crown of a roll has a direct influence on the roll gap and this on the flatness of the strip to be rolled. If this influence is not considered, the increased crown with increasing roll heating would initiate center waves in the strip.

Thermal crown can be offset in advance by adequate roll grinding and preheating of the roll. However, since the process conditions are not constant, deviations in thermal crowning must be considered to achieve optimum flatness.

### 3.5 Table of input and output data

The following table lists the necessary input data for the thermal crown model. Roll data are listed using the example of a work roll. All inputs are initially to be transferred as scalar values. If necessary, the dimensions of the physical constants can be increased to better represent the different roll materials within the rolls, for example. In the same way, the strip temperature can also be transferred as a profile, which only requires slight adjustments in the implementation. The essential output variable is a vector containing the thermal crown. All other data can also be passed on to the outside, just like the temperature profiles of the rolls. This flexibility is also required for the interconnection of the partial models.

**Table 3 - Input data of the thermal crown model**

Input data	Description	Format / Info	Example input	Unit
ts	sample time	double	1	s
<b>Constants</b>				
CONSTANT_k	Thermal conductivity	double	47	W/m/K

<b>CONSTANT_rho</b>	Density	double	8000.0	kg/m <sup>3</sup>
<b>CONSTANT_c</b>	Heat capacity	double	450.0	kJ/kg/K
<b>CONSTANT_beta</b>	Thermal expansion coefficient	double	11.8e-6	1/K
<b>Common width coordinates</b>				
<b>width_t.xa</b>	Begin	double	-1.0	m
<b>width_t.xe</b>	End	double	1.0	m
<b>width_t.xs</b>	Step size	double	0.01	m
<b>Roll description (Values: example work roll)</b>				
<b>roll.cs</b>	Contact to strip	binar	1	1
<b>roll.or</b>	Contact to another roll	binar	1	1
<b>roll.wc</b>	Water cooling	binar	1	1
<b>roll.ac</b>	Air cooling	binar	1	1
<b>roll.T0</b>	Begin temperature	double	20.0	C°
<b>roll.xe</b>	Radius: End	double	0.5	m
<b>roll.xs</b>	Radius: Step size	double	0.01	m
<b>roll.xb</b>	Roll width	double	1.2	m
<b>roll.lf</b>	Length of flattening (contact to another roll)	double	0.002	m
<b>roll.alpha</b>	Heat transfer coefficient (contact to another roll)	double	1000.0	W/K/m <sup>2</sup>
<b>roll.xcvc</b>	CVC-shift	double	0.02	m
<b>Air cooling of rolls (Values: example of one work roll)</b>				
<b>air.h</b>	Heat transfer coefficient to rolls	double	25.0	W/K/m <sup>2</sup>
<b>air.T</b>	Air temperature	double	20.0	C°
<b>Strip data</b>				
<b>strip.alpha</b>	Heat transfer coefficient to rolls	double	1000.0	W/K/m <sup>2</sup>
<b>strip.temperature</b>	Strip temperature	double	800.0	C°
<b>strip.xb</b>	Strip width	double	0.8	m
<b>strip.xa</b>	Strip position	double	0.0	m
<b>strip.h0</b>	Entry thickness	double	0.004	m
<b>strip.h1</b>	Exit thickness	double	0.002	m
<b>strip.v</b>	Strip speed	double	1.0	m/s

**Table 4 - Output data for the thermal crown model**

Output data	Description	Format / Info	Example output	Unit
roll.u[]	Thermal crown	double vector	0.0001 (as maxval)	m
roll.T[][]	Roll Temperature	double matrix	20.0 (beginning)	C°
roll.dqdt[][]	Roll heat flow	double matrix	0.0 (beginning)	W

## 4 Coiling and de-coiling model

### 4.1 General description of the model

The coiling process after hot rolling is a process that may affect the strip shape. During coiling, the strip is bent in tension over the pinch roll. Strip deformation in coiling is similar to the de-formation that occurs during levelling [1]. In levelling, the material is bent over a roll of sufficiently small diameter to cause plastic deformation in the material. The bottom pinch roll, in this case, has a relatively small diameter, usually around 0,5m, and serves the same purpose. When the strip is bent in tension over the pinch roll, it undergoes non-uniform through-thickness plastic deformation with the maximum tensile deformation at the top surface. Such a strain distribution creates positive coil set and helps to keep the coil tight by minimizing the springback effect [2].

The analysis within the present project has been done by physically based approaches, taking the strip thickness profile and the coiling tension into account to calculate coil stresses and deformations, as well as by data-based methods, taking the measured flatness at the exit of the cold mill coiler and at the entry of the galvanizing line into account.

The flatness model for coiling and de-coiling consists of three sub-models:

- Coiling model.
- Air-cooling model.
- De-coiling model.

#### ***Model of stress-strain behavior of the material***

For the calculation of the resulting stresses the material properties described by the stress strain curve of the material have to be considered. The stress-strain curve at elevated temperatures [4, 5]**Error! Reference source not found.****Error! Reference source not found.****Error! Reference source not found.** has been given by the following equations:

$$\sigma_F(\varrho, \varphi, \dot{\varphi}) = A(\varrho, \dot{\varphi}) * (\varphi - p_0)^{B(\varrho)}$$

*Eq. 4-1*

with the material depending on parameters:

$$A(\vartheta, \dot{\varphi}) = a_0 + a_1\vartheta + a_2 * \log \dot{\varphi} + a_3\vartheta \log \dot{\varphi} \quad B(\vartheta) = b_0 + b_1\vartheta$$

Eq. 4-2

The given relation is valid for reductions  $\varphi > 0.002$ . The transition from the quasi-elastic deformation to the plastic deformation is defined at the reduction  $\varphi = 0.002$ . The method of modelling the curve in the complete elastic-plastic region is schematically shown in **Figure 6**.

$$\sigma_F(\varphi, \dot{\varphi}, T) = \begin{cases} E(T)\varphi & \varphi \leq \varphi_s \\ m(\varphi - \varphi_g) + \sigma(\varphi_g, \dot{\varphi}_g, T) & \varphi_s < \varphi \leq \varphi_g \\ \sigma_F(\varphi, \dot{\varphi}, T) & \varphi_g < \varphi \end{cases}$$

with [Error! Reference source not found.]

$$m = \left. \frac{d\sigma_F(\varphi, \dot{\varphi}, T)}{d\varphi} \right|_{\varphi_g, \dot{\varphi}_g, T}$$

$$\dot{\varphi} = \frac{\varphi V}{x}$$

$$\varphi_s = \frac{-m\varphi_g - \sigma(\varphi_g, \dot{\varphi}_g, T)}{E(T) - m}$$

$$E(T) = 2.14 \times 10^5 - 52T - 4.7 \times 10^{-2} T^2$$

Eq. 4-3

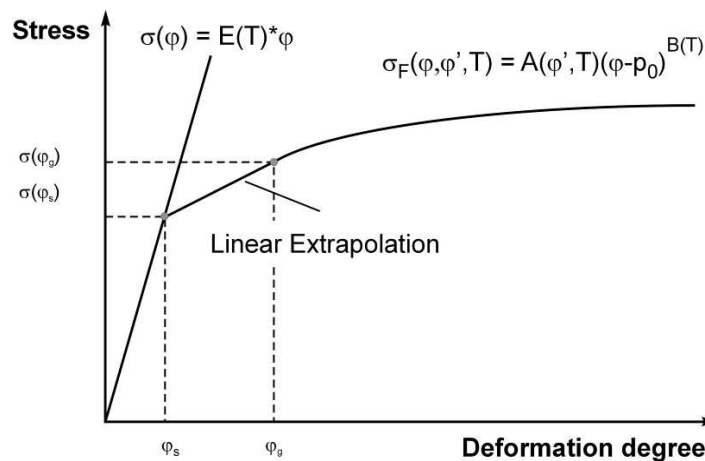


Figure 6. Model of the stress-strain-curve in the complete elastic-plastic region

**Model of strip deformation by the coiler tension**

The calculation starts with an assumed flatness profile of the strip exiting the last stand to which no coiler tension is applied:

$$IU = \frac{L(x) - L_0}{L_0} 10^5 \qquad \varepsilon = \frac{L(x) - L_0}{L_0}$$

Eq. 4-4

The relation between the true strain  $\varphi$  and the local elongation  $\varepsilon$  is given by:

$$\varphi = \ln\left(\frac{L}{L_0}\right) = \ln(\varepsilon + 1) \approx \varepsilon$$

Eq. 4-5

Stress in the outer lap

The stress in the outer lap of the coil as seen in **Figure 7** is mainly induced by

- Strip crown.
- Strip flatness.
- Strip tension.
- Bending of the strip around the coil.

This will be described in some details in this paragraph.

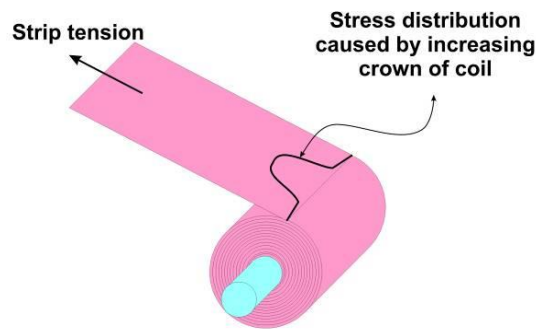


Figure 7. Effect of strip crown on the shape of the coil and on the stress distribution

The strip crown may be described by

$$h(z) = h_0 \left(1 - \alpha \left(\frac{|z|}{(w/2)}\right)^n\right)$$

Eq. 4-6

where

$h_0$  is the nominal thickness,  $\alpha$  the crown ratio (0.5...2 %), and  $N$  the crown exponent (2, 4, 6).

The radius of the coil after  $i$  windings

$$R(z, i) = R_0 + i h(z)$$

Eq. 4-7

The tangential strain of winding  $i$  is:

$$\varepsilon_i(z, i, a) = \frac{u_z}{a} = \begin{cases} \frac{R(z, i-1) - a}{a} & R(z, i-1) - a > 0 \\ 0 & R(z, i-1) - a \leq 0 \end{cases}$$

Eq. 4-8

Next the effect of bending the strip around the coil is investigated; see **Figure 8**.

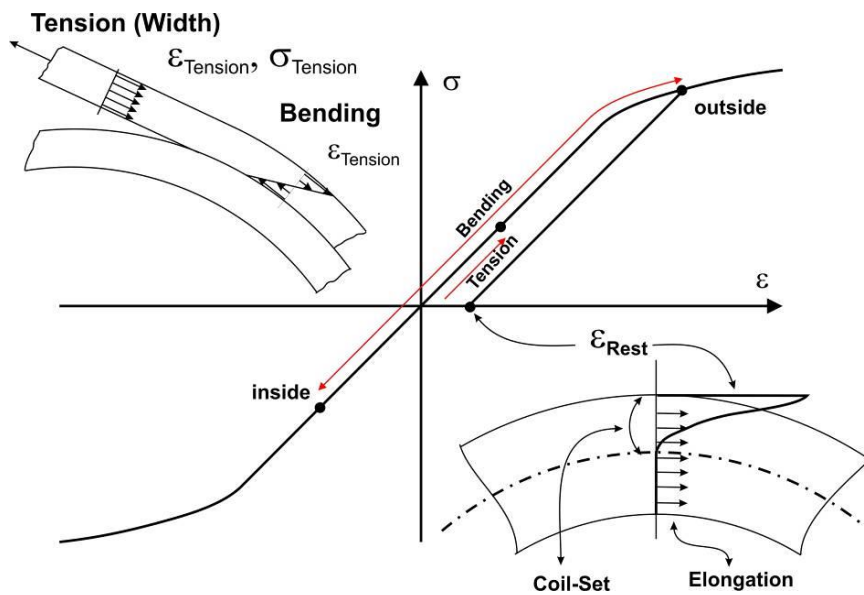


Figure 8. Effect of bending on the stresses across strip thickness

The most inner fibre in strip thickness direction ( $x$ ) will be compressed and the most outer fibre will be stretched.

$$\varepsilon_B(x, z, i) = \frac{x}{2R(z, i)} \quad \text{for } -\frac{h}{2} < x < \frac{h}{2}$$

Eq. 4-9

The total strain caused by shrinking of the outer lap and bending of the lap around the coil is:

$$\varepsilon_{tot}(x, z, i, a) = \varepsilon_t(z, i, a) + \varepsilon_B(x, z, i)$$

$$\sigma_t = E\varepsilon_{tot}$$

**Eq. 4-10**

considering the equilibrium of the force

$$F_z - \int_{-w/2}^{w/2} \int_{-h/2}^{h/2} \sigma_t(z, x, i, a) dx dz = 0$$

**Eq. 4-11**

For the further calculation an average tangential stress is defined as

$$\bar{\sigma}_t(z, i) = \frac{1}{h} \int_{-h/2}^{h/2} \sigma_t(x, z, i, \hat{a}) dx$$

**Eq. 4-12**

### ***Stress in the coil (coil on the mandrel)***

Subsequently the Tangential stress (coil on the mandrel):

$$\sigma_t(r_i, z) = \bar{\sigma}_t(r_i, z) + \sigma'(r_i, z)$$

$$\sigma'_t(r_i, z) = - \left( 1 + \frac{\rho_0^2}{r_i^2} \right) \int_{r_i}^{ra} \bar{\sigma}_t(r, z) \frac{r}{r^2 - \rho_0^2} dr$$

**Eq. 4-13**

and radial stress

$$\sigma_r(r_i, z) = - \left( 1 - \frac{\rho_0^2}{r_i^2} \right) \int_{r_i}^{ra} \bar{\sigma}_t(r, z) \frac{r}{r^2 - \rho_0^2} dr$$

**Eq. 4-14**

in the coil is calculated due to the pressure of the out lap. In this case the coil is still on the mandrel.

### ***Stress in the coil (coil off the mandrel)***

If the coil is taken off the mandrel the stress within the coil will be redistributed because the pressure between the mandrel and the inner lap will disappear. Therefore, the tangential stress is given by:

$$\sigma_{t,relax}(r, z) = \sigma_t(r, z) - \tilde{\sigma}_t(r, z)$$

$$\tilde{\sigma}_t(r, z) = -\sigma_r(R_0, z) \frac{R_0}{R_A^2 - R_0^2} \left( 1 + \frac{R_A^2}{r^2} \right)$$

**Eq. 4-15**

and radial stress is given by

$$\sigma_{r,relax}(r, z) = \sigma_r(r, z) - \tilde{\sigma}_r(r, z)$$

$$\tilde{\sigma}_r(r, z) = -\sigma_r(R_0, z) \frac{R_0}{R_A^2 - R_0^2} \left( 1 - \frac{R_A^2}{r^2} \right)$$

Eq. 4-16

This model has been implemented in MATLAB for offline use. To speed up the computation, it is planned to transfer the model to python or C.

## 4.2 References/source of the model

The model has been partly extracted from a previous project at BFI called LINECOP (RFS-PR-50120). Here the model has been developed for a cold rolling mill. Adaptations for the use in hot rolling will be done by BFI with concrete steps planned, that will be taken. Below a enumeration of all sources used to develop the model is given.

- [1] Gevers P., Tamler H.W. (2001): Internal Stress and Flatness Evolution after Hot Strip Mill. EUR 19874 EN, 2001, pp. 85.
- [2] Nikitenko E., Gris B.C. (2009): Mechanism of post-rolling deterioration in hot band flat-ness during coiling. Iron & Steel Technology, October, pp. 60–63.
- [3] Bernd Berger (1975): The elastic deformation of the rolls from the four-high stand system and the influence of the roll bending on the shape of the roll gap. VDEh-Betriebsforschungsinstitut (BFI).
- [4] Jäckel I., Lommatzsch J. (1989): Spezielle Untersuchungen zur Warmumformfestigkeit ausgewählter Stähle im Bereich kleiner Umformgrade. Neue Hütte 34:8.
- [5] Jäckel I. (1992): Beitrag zur Analyse des Walzens von Vollquerschnitten unter besonderer Berücksichtigung umformwirksamer Längszüge. Verlag Stahleisen, Umformtechnische Schriften, Bd. 36.

## 4.3 Quality of calculation

A qualitative evaluation of the calculated results of the model has been performed in course of LINECOP. Here was concluded that the simulated flatness matches the measured flatness good (at least qualitatively) for the cold rolling process. Since the Temperature of the steel in the coiling process in hot rolling is much warmer, the length of the coiled steel plate also differs, introducing a higher compression acting on the inner layers of the coil after cooling. Additionally the outer part cools faster than the inner, which introduces significant differences in pressure distribution. The current model must be adapted to take this difference between hot and cold rolling into account.

These influences are planned to be included with physics infused neural networks. With these adaptations implemented into the model, a direct improvement for the quality of the model is expected for cold rolling and in case of hot rolling all occurring additional effects should be seen in the simulation as well.

#### 4.4 Influence on flatness

The coiling and decoiling process heavily affect the strip flatness. A typical central observation is that post-rolling flatness often shows edge waves at the head of the strip, but these disappear over the strip length, and are overtaken by center buckles. A possible explanation for this has been acquired in course of the previous project LINECOP for which the model originally was invented. Here the edge waves at the head of the strip can be explained by the mandrel profile which elongates the strip edges during the first few laps of the coil. The mandrel profile will be compensated through the ring coil set. The coil set is caused by the strip crown. After 20–30 laps, the mandrel profile is fully compensated by the coil set, so that the edge waves disappear.

As the coil set increases with increasing coil diameter, the center of the strip will be elongated. Therefore, center buckles are showing up. This effect depends on the material strength and the strip tension. For cold rolling this peak in flatness in the middle due to crown set can be observed in the first third of the coil. For hot rolling this peak shifts towards the last third because of reasons stated above.

#### 4.5 Table of input and output data

All the variables used as an input for the calculation of the coiling and decoiling model are listed in the table down below. The table contains information about the data type, an example input that can be used to run the model and the corresponding unit. As an output the simulated flatness is given.

*Table 5 - Input data for the coiling and decoiling model*

Input data	Format / Info	Example input	Unit
Fz	Strip tension	10,84	kN
h(z)	Strip crown thickness profile	array of size(W) [0.505,...,0.505]	
n	exponent used in h(z)	2, 4, 6	
$\alpha$	Crownparameter	0.01	
T0	Ambient temperature	[20 20 20 20 20] interpolated on size(W)	°C
T1	Temperatur of the strip before cooling	[20 21 22 21 20] interpolated on size(W)	°C
P1	Flatness of strip before cooling	[20*C1 0 5 0 20*C1] interpolated on size(W)	IUnits

T2	Temperatur of the strip after cooling	[19 20 21 20 19] interpolated on size(W)	°C
R0	mandrel inner radius	230	mm
rho	mandrel outer radius	380	mm
W	Contact points over the bandwidth	array of size 51: [-0.625,...,0.625]	mm
X	Distance between last stand and cooling	11	m
V	Bandvelocity	10	m/s
Nring_max	Number of laps contained in the coil	1089	

*Table 6 - Output data for the coiling and decoiling model*

Output data	Format / Info	Example output	Unit
$\sigma$	Stress profile of the coil	array of size 51: [...]	$\frac{kN}{mm^2}$
P	Flatness profile of the band	array of size 51: [...]	IUnits
T	Temperature profile	array of size 51: [20,...,22,...,20]	°C
W	Contact points over the bandwidth	array of size 51: [-0.625,...,0.625]	mm

## 5 Rheological model

A crucial aspect in the rising of plate shape defects is the rheological behaviour of the material being processed (hot plastic flow): in fact, the plasticity characteristics of the material influence the instability parameters that determine the flatness defects (waviness) in the rolled products. The yield stress of the rolled material during the production can't be measured in any way, except in an indirect mode, so that a first-principal model describing the yield stress is required for its evaluation.

## 5.1 General description of the model

In a usual and rather effective approach, the yield stress of the material can be mainly related to the influence of three fundamental variables:

- temperature
- strain
- strain rate

Therefore, the intrinsic plane strain material yield stress is function of the average values of strain  $\varepsilon$ , strain rate  $\dot{\varepsilon}$  and temperature  $T$  of the material in the roll-gap.

$$\mathbf{k}_m = \mathbf{k}_m(\varepsilon, \dot{\varepsilon}, T)$$

*Eq. 5-1*

Such quantities are correlated through a suitable formulation in the form of the product of exponential functions of each above quantity.

### 5.1.1 Average plate strain and strain rate in the roll gap

To calculate the yield stress of the material under deformation in the roll gap, during hot rolling of flat product, the knowledge of the parameters affecting the material behaviour during plastic deformation is needed: temperature, mean strain and strain rate. With the assumption of uniform plane strain deformation of the material in the roll gap, the mean strain is calculated as in the following:

$$\varepsilon = \int_0^\alpha \frac{dh_g}{h_g} = \ln \left( \frac{h_i}{h_{i+1}} \right)$$

*Eq. 5-2*

where:  $h_g$  is the strip thickness in the point corresponding to the generic angle  $\alpha$ ,  $h_i, h_{i+1}$  are the entry and exit strip thicknesses in the  $i$ -th pass and  $\vartheta$  is the contact angle.

As in the previous case, with the assumption of uniform plane strain deformation of the material in the roll gap, it can be assumed:

$$\dot{\varepsilon}_g = \frac{dh_g/dt}{h_g} = \frac{1}{h_g} \frac{dh_g}{d\vartheta} \frac{d\vartheta}{dt}$$

*Eq. 5-3*

where  $\dot{\varepsilon}_g$  is the strain rate of the material at the generic contact angle  $\theta$ .

Taking into account that the rotation speed, in [rad/sec], can be calculated as:

$$\frac{d\vartheta}{dt} = \frac{2\pi N}{60}$$

*Eq. 5-4*

where  $N$  is the revolution speed in terms of [rev/min], it is:

$$\dot{\varepsilon} = \frac{1}{\alpha} \int_0^\alpha \dot{\varepsilon}_\theta \, d\theta = \frac{1}{\alpha} \int_0^\alpha \frac{1}{h_g} \frac{dh_g}{d\theta} \frac{d\theta}{dt} \, d\theta = \frac{1}{\alpha} \frac{2\pi N}{60} \ln\left(\frac{h_i}{h_{i+1}}\right)$$

Eq. 5-5

Considering the contact angle  $\alpha = \sqrt{R\Delta h} / R$  and substituting in the previous equation it can be written:

$$\dot{\varepsilon} = \frac{2\pi N}{60} \sqrt{\frac{R}{\Delta h}} \ln\left(\frac{h_i}{h_{i+1}}\right)$$

Eq. 5-6

Where  $\dot{\varepsilon}$  is the mean strain rate of the material under deformation in the roll gap and  $N$  is the roll revolution speed in rpm.

### 5.1.2 Material constitutive equation

To calculate the steel plate resistance to plastic deformation (material flow stress, expressing the rheological behaviour) the following constitutive equation, function of temperature, average strain and strain rate, is used:

$$k_m = k_{f0} e^{-m_1 T} \varepsilon^{m_2} e^{-m_{22} \varepsilon} \dot{\varepsilon}^{m_3}$$

Eq. 5-7

where:

$\varepsilon$	average strip strain in the roll bite	[-]
$\dot{\varepsilon}$	average strip strain rate in the roll bite	[sec <sup>-1</sup> ]
$T$	average strip temperature in the roll bite	[°C]
$k_{f0}$	Base material yield strength	[N/mm <sup>2</sup> ]
$m_1, m_2, m_3, m_{22}$	Constitutive equation coefficients	

## 5.2 References/source of the model

The theory of the model is mainly based on the following book section:

Landolt-Börnstein - Group VIII Advanced Materials and Technologies, “Numerical Data and Functional Relationships in Science and Technology”, M. Spittel, T. Spittel (auth.), H. Warlimont (eds.) – Vol 2, “Materials” – Subvolume C, “Metal Forming Data” – Part I, “Ferrous alloys”

### 5.3 Quality of calculations

The calibration of the coefficients inside the equations expressing the material rheological behavior is performed starting from the process data and using the formulation of the rolling force in an inverse way; thereby, an information about the actual yield stress during the rolling is obtained and its value is used to calibrate the coefficients. In this way, for each material for each material for which process data, available in sufficient numbers and expressing a wide range of final thicknesses and widths, it is possible to improve the quality and accuracy of the calculation result.

### 5.4 Influence on flatness

The rheological behaviour of the material being processed is a crucial aspect in the rising of plate shape defects: in fact, the plasticity characteristics of the material (hot plastic flow) can strongly influence the instability parameters that determine the flatness defects (waviness) in the rolled products.

### 5.5 Table of input and output data

All the variables used as an input for the rheological model are listed in the table down below. The table contains information about the data type, an example input that can be used to run the model and the corresponding unit. As an output, the calculated flow stress is given.

*Table 7 - Input data of the rheological model*

<b>Input data</b>	<b>Format / Info</b>	<b>Example input</b>	<b>Unit</b>
Width	Plate width	2500, 3000, ...	mm
EntryThickness	Plate entry thickness	From 66 to 35 mm in the finishing stage	mm
ExitThickness	Plate exit thickness	From 25 to 8 mm in the finishing stage	mm
RollingForce	Rolling separation force	From 25000 to 40000 kN in the finishing stage	kN
RollingSpeed	Rolling speed	From 1.5 to 3 m/s in the finishing stage	m/s
WRDiameter	Diameters of the work rolls	970, 990, ...	mm
AvTemperature	Average plate temperature in the roll-gap	From 950 to 750 °C in the finishing stage	°C

SteelGrade	Steel grade for the current plate	String expressing the steel grade (RG18, QG15, S355...)	-
------------	-----------------------------------	---	---

*Table 8 - Output data of the rheological model*

<b>Output data</b>	<b>Format / Info</b>	<b>Example output</b>	<b>Unit</b>
plateYieldStress	Plate yield stress	180, 220, 250, ...	MPa

## 6 Plate temperature evolution model

The strip temperature is an important parameter to be taken into account during the rolling schedule calculation due to its influence on the strip material yield strength and the metallurgical requirements related to the finishing rolling temperature.

The rolling temperature model calculates the bar/strip temperature evolution during all the rolling phases, as a function of the rolling parameters (strip thicknesses and width, rolling forces, rolling speeds, radiation and convection) and steel strip and work roll material thermo-physical properties (density, specific heat, thermal conductivity, emissivity).

### 6.1 General description of the model

An algorithm, based on the finite difference technique, for an accurate calculation of the strip temperature evolution during rolling is included in the set-up model. It evaluates the temperature evolution through the bar/strip thickness, in the middle of its width. The main characteristics of the thermal model are listed below:

- mono-dimensional, finite difference schematization
- implicit solution of the heat conduction equation (Crank-Nicolson method)
- boundary conditions (radiation, contact with the work rolls, cooling due to the work roll cooling water, inter-stand cooling)
- non-linearly thermal dependent strip properties (density, specific heat, heat conduction, diffusivity)
- generation of deformation heat in the roll bite.

The bar/plate thickness is subdivided into elements and only half thickness is taken into account, considering the symmetry plane in the mid-thickness. The grid dimensions are selected with variable steps: shorter steps next to the strip surface and larger steps inside, toward the symmetry plane.

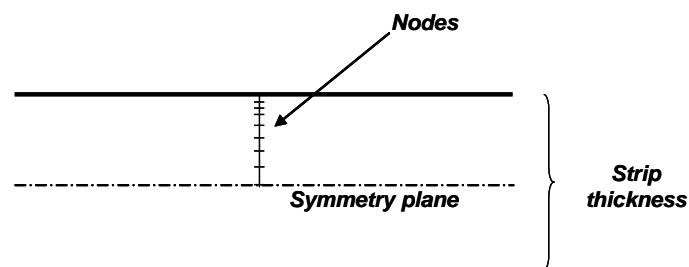


*Figure 9 Mesh elements in the mono-dimensional finite difference solution of the heat conduction equation through the bar/strip thickness*

#### 6.1.1 Finite difference solution of the heat conduction equation – The Crank-Nicolson method

The heat conduction equation to calculate the temperature evolution (Fourier equation) in the nodes along the half strip thickness is:

$$\frac{\partial T}{\partial t} = \alpha(T) \frac{\partial^2 T}{\partial y^2} + \frac{Q_{def}}{\rho c_p}$$

Eq. 6-1

where:

$T$	nodes temperatures	[°C]
$t$	time	[sec]
$\alpha = \alpha(T)$	strip material temperature dependent diffusivity	[m <sup>2</sup> /sec]
$\rho = \rho(T)$	strip material temperature dependent density	[kg/m <sup>3</sup> ]
$c_p = c_p(T)$	strip material temperature specific heat	[J/(kg°C sec)]
$y$	coordinate of the nodes	[m]
$Q_{def}$	deformation heat	[J/( m <sup>3</sup> sec)]

The finite difference technique is a method for solving differential equations by means of the subdivision of the continuous space into elements, calculating the values of the unknown variables on the nodes of the resulting mesh.

Several methods are well known for the solution of the Fourier equation, giving a good approximation of the exact solution. Nevertheless, a lot of them have the inconvenience of the constraint of small time steps needed to perform transient calculations avoiding numerical instabilities and the consequent lack of convergence, giving rise to unacceptable large computing time for real time calculation.

Therefore the finite difference, implicit Crank-Nicolson method has been selected and used to solve equation [5.1].

It is an unconditionally stable method, with the advantage to make possible the thermal simulation with a reduced number of time steps, allowing to save computing time, without badly affecting the precision of the temperature prediction.

According to the Crank-Nicolson method, the temperatures in the grid nodes are calculated, in the case of variable grid size, with the following formula:

$$\frac{T_i^{n+1} - T_i^n}{\Delta t} = \frac{\alpha}{2\Delta y_m} \left( \frac{T_{i-1}^{n+1}}{\Delta y_{i-1}} + \frac{T_{i+1}^{n+1}}{\Delta y_i} - \frac{T_i^{n+1}}{\Delta y_{i-1}} - \frac{T_i^{n+1}}{\Delta y_i} + \frac{T_{i+1}^n - T_i^n}{\Delta y_i} - \frac{T_i^n - T_{i-1}^n}{\Delta y_{i-1}} \right) + \frac{Q_{def}}{\rho c_p}$$

Eq. 6-2

$$\Delta y_m = \frac{\Delta y_{i-1} + \Delta y_i}{2}$$

Where:

is the average size of adjacent elements. The index  $i$  indicates the  $i$ -th node and the index  $n$  indicates the  $n$ -th time step.

Equation [5.2] can be written as in the following, with the terms including the unknown temperatures of the  $(n+1)$ -th time step on the left side and the known temperature of the  $n$ -th time step on the right side:

$$-\frac{\chi_f}{\Delta y_{i-1}} T_{i-1}^{n+1} + T_i^{n+1} \left( 1 + \frac{\chi_f}{\Delta y_{i-1}} + \frac{\chi_f}{\Delta y_i} \right) - \frac{\chi_f}{\Delta y_i} T_{i+1}^{n+1} = T_i^n + \chi_f \left( \frac{T_{i+1}^n - T_i^n}{\Delta y_i} - \frac{T_i^n - T_{i-1}^n}{\Delta y_{i-1}} \right) + \frac{Q_{def}}{\rho c_p}$$

Eq. 6-3

With:

$$\chi_f = \frac{\alpha \Delta t}{2 \Delta y_m}$$

Hence it is possible to calculate the temperatures on the grid nodes solving the system of equations [5.3], where the unknowns are the temperatures of the nodes at the next  $(n+1)$ -th time step.

Writing:

$$B = -\frac{\chi_f}{\Delta y_{i-1}} \quad \text{coefficient behind the main diagonal}$$

$$D = \left( 1 + \frac{\chi_f}{\Delta y_{i-1}} + \frac{\chi_f}{\Delta y_i} \right) \quad \text{coefficient on the main diagonal}$$

$$A = -\frac{\chi_f}{\Delta y_i} \quad \text{coefficient ahead the main diagonal}$$

$$C = T_i^n + \chi_f \left( \frac{T_{i+1}^n - T_i^n}{\Delta y_i} - \frac{T_i^n - T_{i-1}^n}{\Delta y_{i-1}} \right) + \frac{Q_{def}}{\rho c_p} \quad \text{elements in the constant vector}$$

The temperature on the nodes in the  $(n+1)$ -th time step can be calculated solving a tri-diagonal system of equations.

The system of equations is represented in matrix form, where on the left there is the product between the matrix of the coefficients of the equations and the vector of the unknown nodes temperatures, while on the right there is the vector of the constants of the equations. The other terms of the matrix of the equation coefficients are equal to 0.



- contact between strip and work roll in the roll bite.

## 6.2 References/source of the model

The theory of the model is mainly based on the following paper (and related):

Martha P. Guerrero, Carlos R. Flores, Antonino Perez, Rafael Co-Las: "Modelling heat transfer in hot rolling work rolls," Journal of Materials Processing Technology, vol. 94, pp. 52-59, 1999.

## 6.3 Quality of calculations

The quality and accuracy of calculations is improved by means of a calibration of some tuning parameters that can be set on the basis of the rolling data, using the measurements of the pyrometers positioned along the production line and performing a matching between the measured and calculated plate surface temperatures. An example of such tuning parameters is the coefficient expressing the contact percentage between the hot plate and the work rolls: such quantity is responsible of the heat transfer between the piece and the rolls and it affects the changing in the surface temperature during the rolling, so it can be used to perform a regulation of the temperature drop in the roll-gap, targeting the measured exit temperature.

## 6.4 Influence on Flatness

Plate temperature is one of the most important features affecting the rheological behaviour of the material and consequently it is an important variable in the evaluation of the causes that determine the rising of flatness defects: when the value of the temperature is not available from the on-field measurements, a model assessing the thermal evolution is needed, in order to complete the information about the plate during the working. Therefore, a principal model was developed to evaluate this fundamental parameter.

## 6.5 Table of input and output data

All the variables used as an input for the plate temperature evolution model are listed in the table down below. The table contains information about the data type, an example input that can be used to run the model and the corresponding unit. As an output, the calculated current values of the temperatures across the nodes dividing the plate thickness are given.

*Table 9 - Input data of the plate temperature evolution model*

Input data	Format / Info	Example input	Unit
entryWidth	Plate width at the entry of the stand	2500, 3000, ...	mm

exitWidth	Plate width at the exit of the stand	2500, 3000, ...	mm
EntryThickness	Plate entry thickness	From 66 to 35 mm in the finishing stage	mm
ExitThickness	Plate exit thickness	From 25 to 8 mm in the finishing stage	mm
RollingForce	Rolling separation force	From 25000 to 40000 kN in the finishing stage	kN
RollingSpeed	Rolling speed	From 1.5 to 3 m/s in the finishing stage	m/s
WRDiameter	Diameters of the work rolls	970, 990, ...	mm
WRTableLength	Work roll table length	4800	mm
WRPoissonCoef	Work roll Poisson coefficient	0.25, 0.30, ...	-
WRYoungMod	Work roll Young modulus	180, 210, ...	GPa
numPasses	Number of passes	7, 9, ...	-
numStartNodes	Number of starting nodes subdividing the plate thickness	7	-
entryBarLengths	Bar length at the entry of the stand	5000, 8000, ...	mm
exitBarLengths	Bar length at the exit of the stand	10000, 12000, ...	mm
headBarThreadSpeeds	Threading speeds of the bar heads at the exit of each pass	1.5, 2, ...	m/s
tailBarExitSpeeds	Final speeds of the tail of the bar at the exit of each pass	3, 3.5, ...	m/s
speedUpAccelerations	Bar speed up acceleration	0.5	m/s <sup>2</sup>

maxHighBarSpeed[]	Max high bar speed after speed up acceleration	3.5	m/s
tailSlowDownDecelerations[]	Bar slow down decelerations (positive acceleration value is considered)	0.5	m/s <sup>2</sup>
relHeadDistanceRefSect	Initial relative distance of the reference section from the bar head	12	m
reverseTime[]	Time for speed reverse	5, 8, 20, ...	s
avBarSpeed	Average transfer bar speed at the entry roller table, before the 1st pass	1, 2, ...	m/s
plateRotationFlag[]	Flag to select the rotation of the plate (90°) from the entry of the 1st to the exit of the last passes	0, 1	-
entryRadZoneLength	Length of the entry table, under radiation, before the descaler at the entry of the stand before the first pass	10	m
idleTimeEntryRadZone	Idle waiting time of the bar ahead the entry table of the descaler before the mill stand	10	s
standardReverseTimeNoRot	Standard reverse time interval among the inter-passes for speed recersing and bar centering without rotation	5	s
standardReverseTimeRot	Standard reverse time interval among the inter-passes for speed	10	s

	reversing and bar centering with rotation		
descalerFlag	Flag to determine the presence of a descaler at the entry of the pass	0, 1	-
desc1stRadZone	Length of the 1st zone under the descaler before the 1st impinging jet	0.02, 0.05, ...	m
desc1stJetFlag	1st descaler jet operating flag	0, 1	-
desc1stJetLength	Length of the 1st descaler jet impinging on the bar surface	0.02, 0.05, ...	m
desc1stJetWaterHc	Average heat exchange coefficient in the contact between the strip and the 1st jet descaling water	15000, 20000, ...	J/m <sup>2</sup> /°C/s
desc2ndRadZone	Bar length of the zone under the descaler between the 1st and 2nd impinging jets	0.02, 0.05, ...	m
desc2ndJetFlag	2nd descaler jet operating flag	0, 1	-
desc2ndJetLength	Length of the 2nd descaler jet impinging on the bar surface	0.02, 0.05, ...	m
desc2ndJetWaterHc	Average heat exchange coefficient in the contact between the strip and the 2nd jet descaling water	15000, 20000, ...	J/m <sup>2</sup> /°C/s
desc3rdRadZone	Bar length of the 3rd zone under the descaler after the 2nd impinging jet	0.02, 0.05, ...	m

descStand	distance between the descaler and the axis of the stand	3, 4, ...	m
descalerWaterTemp	Average temperature of the descaling water	35, 45, ...	°C
avExtTemp	Average ambient temperature between the crop shear and the descaler	20, 35, ...	°C
avExtEmiss	Average ambient emissivity between the crop shear and the descaler	0.7, 0.9, ...	-
EntryWCplateLength	Plate length cooled by the work roll water cooling at the entry of the mill stands	0.02, 0.03, ...	m
ExitWCstriplength	Plate length cooled by the work roll water cooling at the exit of the mill stands	0.02, 0.03, ...	m
avROTextTemp	Average ambient temperature along the entry and exit roller table	20, 35, ...	°C
avROTextEmiss	Average ambient emissivity along the entry and exit roller table	0.7, 0.9, ...	-
exitStandPyromDistance	Distance between the stand and the exit pyrometer on the roller table	3, 5, ...	m
wrWaterCTemp	Average temperature of the work roll cooling water	35, 45, ...	°C
wrTemp	Average temperature of the work rolls	80, 90, ...	°C

wrWaterCHc	Average heat exchange coefficient in the contact between the plate and the work roll cooling water	200, 250, ...	J/m <sup>2</sup> /°C/s
kContact	Multiplier coefficient of the roll/strip contact heat exchange coefficient	Ranged between 0 and 1	-
initT	Bar initial temperature	1150, 1180, ...	°C
steelYieldStress	Steel yield stress, evaluated from the rheological model of the current material	190, 250, 270, ...	MPa
wrDensity	Work roll shell density	2500, 2700, ...	kg/m <sup>3</sup>
wrThermCond	Work roll shell thermal conductivity	22, 30, ...	J/m/sec
wrSpHeat	Work roll shell specific heat	450, 500, ...	J/kg/°C
wrAlpha	Work roll shell linear expansion coefficient	0.000012, 0.000015,...	1/°C
shellThickness	Thickness of the work roll shell	15, 20, ...	mm
wrCoreDensity	Work roll core density	2500, 2700, ...	kg/m <sup>3</sup>
wrCoreThermCond	Work roll core thermal conductivity	22, 30, ...	J/m/sec
wrCoreSpHeat	Work roll core specific heat	450, 500, ...	J/kg/°C
wrCoreAlpha	Work roll core linear expansion coefficient	0.000012, 0.000015,...	1/°C
maxSpecRollForce	Max. allowed rolling force per unit strip width	12, 15, ...	N/mm
length	Length of the run-out table	110, 140, ...	m

diaRolls	Diameter of the rolls of the run-out table	250, 330, ...	mm
thickRolls	Thickness of the rolls of the run-out table	25, 30, ...	mm
intPassRolls	Inter-pass between the rolls	250, 300, ...	mm
condRolls	Conductivity of the rolls of the run-out table	22, 30, ...	J/(m s °C)
coeffPoissonRolls	Poisson coefficients of the rolls	0.35	-
modYoungRolls	Young modulus of the rolls of the run-out table	180, 210, ...	N/mm <sup>2</sup>
waterRollCoolTemp	Temperature of the water internal cooling of the rolls of the run-out table	35, 45, ...	°C
rollSurfTemp	Average surface temperature of the rolls	180, 200, ...	°C
airTempTop	Ambient air temperature on the top bar surface	25	°C
airTempBot	Ambient air temperature on the bottom bar surface [°C]	25	°C
extTopTemp	External top temperature	35	°C
extBotTemp	External bottom temperature	35	°C
avBarSpeed	Average speed of the plate travelling through the run-out table	3, 3.5, ...	m/s
maxRollerTableSpeed;	Maximum speed of the roller table	4.5	m/s

rollerTableAcceleration	Acceleration of the roller table	0.5	m/s <sup>2</sup>
rollerTableDeceleration	Deceleration of the roller table	0.5	m/s <sup>2</sup>
dummyPass	Dummy pass identifier	0, 1	-
forwardSlip[]	Plate forward slip at the exit of the stands	0.015, 0.025, ...	-
airTemp	Air temperature	18, 35, ...	°C

*Table 10 - Output data of the plate temperature evolution model*

Output data	Format / Info	Example output	Unit
avGapPlateSurfaceTemp	Average temperature of the plate surface in the roll gap	780, 1150, ...	°C
avRollingEntryTemperature	Average temperature of the plate at the entry of the roll gap	780, 1150, ...	°C
avRollingExitTemperature	Average temperature of the plate at the exit of the roll gap	780, 1150, ...	°C
avRollingTemperature	Average plate temperature in the roll gap	780, 1150, ...	°C

## 7 Roll wear model

### 7.1 General description of the model

The work rolls are divided into  $n$  elements across the work roll table length. At each rolling pass it is calculated the wear increments on the elements, due to the contact with the hot rolled steel. The evolution of the work roll wear profile is updated summing at each time step the wear increments.

Wear increment on the  $i_e$ -th roll element:

$$\Delta W_{inc} = a_w \bar{F}_{sp}^{m_w} \frac{L_{strip}}{D_{cil}} \varphi C_{fact}$$

Eq. 7-1

Rolling pressure in the roll bite:

$$\bar{F}_{sp} = 1000 \frac{F_{meas}}{WL_p}$$

Eq. 7-2

Wear updating on the ie-th roll element:

$$W_{wear} = W_{prevWear} + \Delta W_{inc}$$

Eq. 7-3

Where:

$m_w$	roll material dependent wear increment model coefficients
$\varphi$	Wear increment factor
$C_{fact}$	Roll element covering factor

## 7.2 References/source of the model

The theory of the model is mainly based on the following papers (and related):

[1] Y.T. Azene , R. Roy , D. Farrugia, C. Onisa , J. Mehnen and H. Trautmann. - Work roll cooling system design optimisation in presence of uncertainty and constrains," CIRP Journal of Manufacturing Science and Technology, vol. 2, pp. 290-298, 2010.

[2] Corral R.L, Cols R and Prez A. - Modelling the thermal and thermo-elastic responses of work rolls used for hot rolling steel strip," Journal of Materials Processing Technology, vol. 154, pp. 886893, 2004.

## 7.3 Quality of calculations

The quality and accuracy of calculations is improved by means of a calibration of some tuning parameters that can be set on the basis of the rolling data, using a specific roll wear measurements method, performed by detecting the work roll profile (cold after grinding) before the starting of a test

rolling campaign and re-detecting the work roll profile at the work roll dismounting, after waiting for the work rolls cooling at the rolls dismounting; in this way, two tuning parameters (the multiplying coefficient and the exponent inside the roll wear increment equation) are set to target a match with the final measured roll wear. If the results of more campaigns are used, a statistical approach can be adopted.

## 7.4 Influence on Flatness

The work roll wear is a major factor affecting the steel plates shape (mainly flatness and profile because, at the exit of each stand, net of small elastic returns, the plate assumes the shape of the loaded roll-gap. The roll-gap shape is strongly itself by the roll consuming during the rolling, since the contact with the hot plate digs and progressively erodes the cylinders, creating local disturbances of the work roll profile and consequently giving rise to local deformations which, if excessive, can result in flatness defects (waving).

## 7.5 Table of input and output data

All the variables used as an input for the wear model are listed in the table down below. The table contains information about the data type, an example input that can be used to run the model and the corresponding unit. As an output, the calculated current value of the work roll wear is given.

*Table 11 - Input data roll wear model*

Input data	Format / Info	Example input	Unit
timestep	Time step between two consecutive calculations	0.5 s	s
metallnStandFlag	Flat to assess the presence of the steel inside the roll-gap	0; 1	-
Width	Plate width	2500, 3000, ...	mm
EntryThickness	Plate entry thickness	From 66 to 35 mm in the finishing stage	mm
ExitThickness	Plate exit thickness	From 25 to 8 mm in the finishing stage	mm
RollingForce	Rolling separation force	From 25000 to 40000 kN in the finishing stage	kN
RollingSpeed	Rolling speed	From 1.5 to 3 m/s in the finishing stage	m/s

WRDiameter	Diameters of the work rolls	970, 990, ...	mm
WRTableLength	Work roll table length	4800	mm
WRPoissonCoef	Work roll Poisson coefficient	0.25, 0.30, ...	-
WRYoungMod	Work roll Young modulus	180, 210, ...	GPa
WRwearPrev	Work roll wear at the previous time step	0.05, 0.1 mm	mm

*Table 12 - Output data roll wear model*

Output data	Format / Info	Example output	Unit
rollDiaWearUp	Work roll diameter wear (wear in the middle of the work roll table)	0.0005, 0.005, 0.5, ...	mm
wRollwearUp	Total wear along all the roll table length (all the values of the wear profile)	0.0005, 0.005, 0.5, ...	mm
rollDiaWearBt	Work roll diameter wear (wear in the middle of the work roll table)	0.0005, 0.005, 0.5, ...	mm
wRollwearBt	Total wear along all the roll table length (all the values of the wear profile)	0.0005, 0.005, 0.5, ...	mm

## 8 Analytic forming model of levelling process

### 8.1 General description of the model

Normally, the flatness of the material is controlled by the positioning of the rollers and back-up rolls of the levellers, which depends on the skill and experience of the operator.

Fagor's new non-contact flatness control system and closed loop system, will give the operator a reliable tool to assess the flatness of the sheet in real time. The system is easily integrated into the production line to continuously monitor the state of the sheet with great precision.

Additionally, using the flatness quality measurements got from the line, before processing the sheet at levelling machine and based on mathematical calculations, the system will propose to the operator, optimum back-up roll position in order to get high levelling quality.

The purpose of the flatness measuring equipment behind the leveller is to measure local defects of the sheet across its full width and correct the position of the leveller supports to correct these defects.

Local defects in a sheet are created by differences in length between various longitudinal fibers across the width of the sheet. For this reason, the measurement of flatness of the sheet will be made by measuring the relative lengths of fibers in the width of the strip.

For this, the measuring equipment has a double beam laser triangulation equipment (to discriminate the effect of vibration) which is equivalent to having a high number of points located in the width of the band and homogeneously distributed. Through this system, the lengths of fibers in the length of the sheet will be measured, which will allow the map of IUnits in the band to be determined and thus correct those localized areas of the sheet that present a greater number of IUnits.

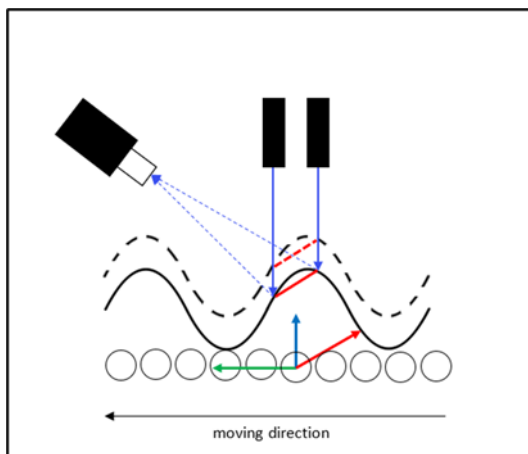


**Figure 11 - Measuring equipment: triangulation**

Fiber lengths between two consecutive points on a fiber can be calculated using the following equation:

$$L = \sum_{i=1}^{i=n} \sqrt{(h_{i+1} - h_i)^2 + v_i \cdot (t_{i+1} - t_i)^2}$$

Eq. 8-1

Where:

$h_i$  is the distance of the sensor to  $i$  point of the sheet

$v_i$  is the speed of the sheet at point  $i$

$t_i$  is the time at point  $i$

$L$  is the real length of the fiber after reading  $n$  points

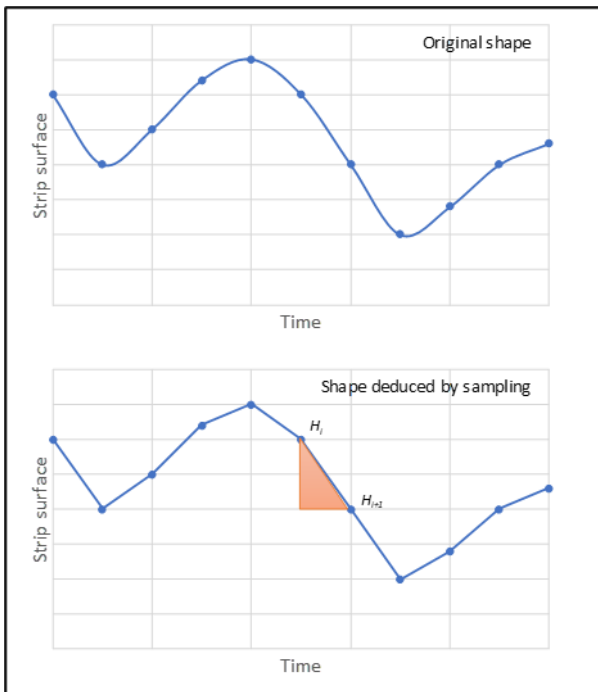


Figure 12 - Fiber length calculation

From the measurement of the fiber lengths in the width of the plate, the strain of the fibers can be determined from the relative lengths between them and the IUnits.

$$\Delta L = L - L_{max}$$

$$\varepsilon = \frac{\Delta L}{L_{max}}$$

$$IU = \varepsilon \cdot 10^5$$

Eq. 8-2

Fibers where the relative strain or elongation is zero or lower must be elongated so that they reach the same elongation/strain value as the rest of the fibers. This is achieved by selective displacement of the back-up rolls.

The back-up rolls will be positioned with the aim of stretching the fibers of the areas of the sheet where there are no waves so that they are equal with the rest. For example, if the sheet has edge waves, the central supports will rise to bend the roller in that area and apply greater deformation to the sheet, thus increasing its length. On the contrary, if we have central bags, it will be the end supports that will rise with the aim of stretching the end areas and equalizing them with respect to the deformation of the central sheet.

The measurement points will be located homogeneously along the width of the band, and these will be associated with the different supports of the machine according to their location. Therefore, depending on the width of the sheet, the corresponding supports will be used to correct the defects based on the measurements made and associated with each of these supports.

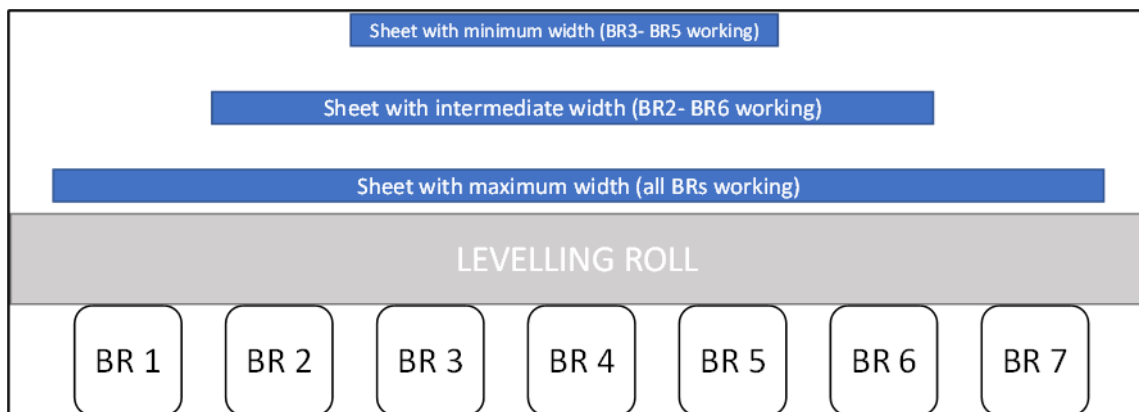


Figure 13 - Width of the band and back-up roll supports.

An analytical model has been developed to calculate the necessary displacement for each support to correct the defects detected with the vision system based on the relative fiber length

Necessary parameters:

Nº of back-up roll supports	n
Distance between back-up roll supports, mm	da
Roll length, mm	Tr
Distance between Edge and Back-up roll supports, mm	Br
Distance between working rolls, mm	p
Sheet thickness, mm	e
Young modulus, MPa	E
% Plasticization by tilting	Pr
yield strength, MPa	Re
Sheet width, mm	W
Radius of curvature with support	Rc
Radius of curvature without support	Rc0
Setting without support	h0

With these data, the number of useful back-up roll supports will be determined based on the bandwidth:

Nº support	Maximum width (mm)
1	Da + br
3	3*Da + br
5	5*Da + br
7	7*Da + br
9	9*Da + br

For each support, a single deformation value will be analysed (see section...). Specifically, vision software will provide a maximum fiber length value for each support.

$$L_1, L_2, L_3 \dots L_n$$

Eq. 8-3

For each fiber length, the increase in length with respect to the longest fiber, its deformation and its

$$L_{max} = \max(L_i)$$

$$\Delta L_i = L - L_{max}$$

$$\varepsilon_i = \frac{\Delta L_i}{L_{max}}$$

$$IU_i = \varepsilon_i \cdot 10^5$$

Eq. 8-4

IUnits will be calculated.

With these values, the setting increment that each support must carry out and the corresponding plasticisation increment will be determined:

$$\Delta h = \sqrt{\frac{IU \cdot 4 \cdot p^2}{\pi^2 \cdot 10^5}}$$

$$\Delta_{plast} = \left(100 - \left(\frac{Rc \cdot 200 \cdot Re}{E \cdot e}\right)\right) - pr$$

$$Rc = \frac{(\Delta h + h0)^2 + (p/2)^2}{4 \cdot (\Delta h + h0)}$$

$$h0 = 2 \cdot Rc0 - \sqrt{4 \cdot Rc0^2 - (p/2)^2}$$

$$Rc0 = \frac{E \cdot e \cdot (100 - pr)}{200 \cdot Re}$$

Eq. 8-5

## 8.2 References/source of the model

[1] E. Silvestre, "Sheet metal roll levelling optimization by means of advanced numerical models and development of new concepts for last generation materials," Thesis dissertation, Mondragon University, 2015.

## 8.3 Quality of calculation results

As the model is based on mathematical calculations, the quality of the results will be a good approximation of the optimum back-up roll position in order to get high levelling quality.

## 8.4 Influence on flatness

The purpose of the flatness measuring equipment behind the leveller is to measure local defects of the sheet across its full width and correct the position of the leveller supports to correct these defects.

Local defects in a sheet are created by differences in length between various longitudinal fibers across the width of the sheet. For this reason, the measurement of flatness of the sheet will be made by measuring the relative lengths of fibers in the width of the strip.

For this, the measuring equipment has a double beam laser triangulation equipment (to discriminate the effect of vibration) which is equivalent to having a high number of points located in the width of the band and homogeneously distributed. Through this system, the lengths of fibers in the length of the sheet will be measured, which will allow the map of IUnits in the band to be determined and thus correct those localized areas of the sheet that present a greater number of IUnits.

## 8.5 Table of input and output data

*Table 13 - Input data for the levelling model*

Input data	Format/Info	Unit
n	Nº of back-up roll supports	
da	Distance between back-up roll supports	mm
Tr	Roll length	mm
Br	Distance between Edge and Back-up roll supports	mm
p	Distance between working rolls	mm
e	Sheet thickness	mm
E	Young modulus	MPa
Pr	% Plasticization by tilting	
Re	Yield strength	MPa

W	Sheet width	mm
Rc	Radius of curvature with support	mm
Rc()	Radius of curvature without support	mm
h0	Setting without support	

[www.HATFLAT.eu](http://www.HATFLAT.eu)

